

Urodeles Remove Mesoderm from the Superficial Layer by Subduction through a Bilateral Primitive Streak

David R. Shook,¹ Christina Majer, and Ray Keller

Department of Biology, University of Virginia, P.O. Box 400328,
Charlottesville, Virginia 22904-4328

Urodeles begin gastrulation with much of their presumptive mesoderm in the superficial cell layer, all of which must move into the deep layers during development. We studied the morphogenesis of superficial mesoderm in the urodeles *Ambystoma maculatum*, *Ambystoma mexicanum*, and *Taricha granulosa*. In all three species, somitic, lateral, and ventral mesoderm move into the deep layer during gastrulation, ingressing through a “bilateral primitive streak” just inside the blastopore. The mesodermal epithelium appears to slide under the endodermal epithelium by a mechanism we term “subduction.” Subduction removes the large expanse of superficial presumptive somitic and lateral–ventral mesoderm that initially separates the sub-blastoporal endoderm from the notochord, leaving the endoderm bounding the still epithelial notochord along the gastrocoel roof. Subduction may be a common feature of urodele gastrulation, differing in this regard from anurans. Subducting cells constrict their apices and become bottle-shaped as they approach the junction of the mesodermal and endodermal epithelia. Subducting bottle cells endocytose apical membrane and withdraw the tight junctional component cingulin from the contracting circumferential tight junctions. Either in conjunction with or immediately after subducting, the mesodermal cells undergo an epithelial-to-mesenchymal transition. The mechanism by which epithelial cells release their apical junctions to become mesenchymal, without disrupting the integrity of the epithelium, remains mysterious, but this system should prove useful in understanding this process in a developmental context. © 2002 Elsevier Science (USA)

Key Words: endocytosis; Keller sandwich explants; giant sandwich explants; ingression; primitive streak; subduction; *Ambystoma maculatum*; *Ambystoma mexicanum*; *Taricha granulosa*; superficial mesoderm; epithelial–mesenchymal transition; epithelial morphogenesis.

INTRODUCTION

Here, we address the question of how the superficial presumptive mesoderm leaves the surface layer of the gastrula and joins the deep layer during gastrulation of urodele amphibians. Amphibian gastrulation involves involution, or rolling inward of the surface of the embryo (Keller, 1986), to form the lining of the primitive gut cavity (Fig. 1). The tissue that involutes is called the involuting marginal zone (IMZ) and lies between an animal cap consisting of presumptive ectoderm and a vegetal region consisting of presumptive endoderm (Fig. 1). The IMZ consists of a superficial epithelial layer and a deep layer, the latter

often consisting of several layers of mesenchymal cells (Fig. 1). The simplest form of amphibian gastrulation would be the case in which the superficial layer of the IMZ consists of presumptive endoderm and the deep layer consists of presumptive mesoderm (Fig. 1A). In this case, involution of the IMZ brings the mesoderm to lie between an outer layer of ectoderm and an inner layer of endoderm lining the gut cavity (Fig. 1A). However, if part or all of the superficial layer of the IMZ consists of presumptive mesoderm (superficial presumptive mesoderm), this presumptive mesoderm will remain on the topological surface after involution, lining the roof of the gut cavity (Fig. 1B).

All amphibians examined to date, both anurans (Fig. 2A) and urodeles (Fig. 2B), have presumptive mesoderm in the superficial (surface) layer of their pregastrula fate map. Therefore, a process other than involution must bring this superficial component of the mesoderm into the deep layer;

¹ To whom correspondence should be addressed. Fax: (434) 982-5626. E-mail: drs6j@virginia.edu.

we refer to this process as ingression.² Until the ingression of all mesoderm out of the epithelial lining of the primitive gut cavity is completed, the cavity is referred to as a gastrocoel; once the cavity is lined entirely by endoderm, it becomes the definitive archenteron.

In all amphibians, the superficial component of the presumptive notochord first involutes to occupy a region on the roof of the gastrocoel (the notochordal plate) during gastrulation (Fig. 2) and then ingresses into the deep layer from the gastrocoel roof during neurulation (Jordan, 1893; King, 1903; Vogt, 1929; Lofberg, 1974; Lundmark, 1986; Imoh, 1988; Purcell and Keller, 1993; Minsuk and Keller, 1996, 1997; and Shook and Keller, unpublished data).

In contrast to the relative similarity of notochordal ingression, the location, timing, extent, and mechanism of the ingression of presumptive somitic mesoderm are highly variable among amphibians, especially between anurans and urodeles. In anurans, the superficial somitic tissue involutes and extends alongside the notochordal plate on the gastrocoel roof (Fig. 2A). Then, during early to mid-neurulation, the superficial somitic cells between the lateral endodermal crests and the notochordal plate (Fig. 2A, black arrow) begin to ingress (Purcell and Keller, 1993; Minsuk and Keller, 1996, 1997; and Shook and Keller, unpublished data). The anurans have relatively little superficial presumptive somitic mesoderm, ranging from substantial amounts in *Ceratophrys* (Purcell and Keller, 1993) to one to three cells per somite in *Xenopus* (Shook and Keller, unpublished data).

In contrast to the smaller amount in anurans (Fig. 2A), the urodeles have a massive amount of superficial presumptive somitic and lateral-ventral mesoderm, which must be removed during gastrulation (Fig. 2B). At least some presumptive mesodermal cells leave the urodele surface layer just inside the blastopore lip (Vogt, 1929; Holtfreter, 1944; Lewis, 1948, 1952; Lundmark, 1986), as bottle cells. Bottle cells are flask-shaped cells with constricted apices, thin elongated necks, and bulbous basal ends due to basal displacement of cytoplasm. However, the details of this ingression are unknown, largely because it occurs within the complex geometry of the blastoporal lip.

Time-lapse video microscopy of explants of three species of urodele, *Ambystoma maculatum*, *Ambystoma mexicanum*, and *Taricha granulosa*, shows that their superficial presumptive somitic and ventrolateral mesoderm ingresses into the deep layer at its epithelial junction with the sub-blastoporal endoderm in a movement we call "subduction." We describe the mechanism, timing, and pattern of

mesodermal subduction. It involves an epithelial-to-mesenchymal transition (EMT) that includes apical constriction, coupled to the formation of bottle cells and the endocytosis of apical membrane, and ultimately loss of contact with the superficial epithelial layer. Blastoporal subduction resembles the ingression of the corresponding presumptive mesoderm through the mouse or chick primitive streak, where the mesoderm begins in the epiblast, in the same superficial layer with the ectoderm and endoderm (Lawson *et al.*, 1991; Schoenwolf *et al.*, 1992; Psychoyos and Stern, 1996), except that in amphibians it occurs through "bilateral primitive streaks," one on each side of a large mass of yolky vegetal endoderm. We also show that the EMT undergone by subducting cells is autonomous in that it is independent of interaction with endoderm. Our observations define for further study a number of issues about cell biological mechanisms of subduction.

MATERIALS AND METHODS

Embryo Culture and Manipulation

A. maculatum embryos were obtained from local ephemeral riparian pools. *A. mexicanum* embryos were obtained from the Indiana University Axolotl Colony (Bloomington, IN). *T. granulosa* (collected in Corvallis, OR) were a kind gift of Adam Jones. Embryos were dejellied manually, and intact embryos were cultured in 1/5× Steinberg's (1× Steinberg's = 60 mM NaCl, 0.67 mM KCl, 0.34 mM Ca(NO₃)₂ · 2H₂O, 0.83 mM MgSO₄, 10 mM HEPES) or 1/5× Holtfreter's (1× Holtfreter's for urodeles = 120 mM NaCl, 1.2 mM KCl, 1.8 mM CaCl₂, 2.4 mM NaHCO₃) (Rugh, 1948) at 4–25°C. Embryos were staged according to Bordzilovskaya *et al.* (1989).

Explants were made with eyebrow knives and hairloops and cultured in 2/3× Holtfreter's or DFA (Sater *et al.*, 1993), with antibiotic/antimycotic (Sigma No. A-9909) in disposable plastic petri dishes. Petri dishes coated with 1% agarose or media with 0.1% BSA were used to prevent tissue from sticking to the plastic. "Giant sandwich" explants, modified from Keller (1991) and Poznanski *et al.* (1997), and "dorsal isolate" explants, a modification of the "filets" of Minsuk and Keller (1996) or the Wilson explants (Wilson *et al.*, 1989; Wilson, 1990), were made as described in Results.

Time-Lapse Movies

Explants were recorded by using a Hamamatsu or Dage MTI CCD camera and a Scion image capture board, as sequential tif files with NIH Image software (developed by Wayne Rasband, National Institutes of Health; available at <http://rsb.info.nih.gov/nih-image/>). Explants were viewed through a dissection stereomicroscope and illuminated with oblique light from two fiber-optic lamps.

Image Analysis

Object Image (a modification of NIH Image by Norbert Vischer, available at <http://simon.bio.uva.nl/object-image.html>) was used to measure and trace important features in explants. Cells disap-

² We use "ingression" here as a generic term for the movement of cells from the epithelial to the deep layers in amphibians, whether as individuals or as a coherent sheet of cells. This is an expansion of the meaning of ingression from its traditional usage, e.g., as in sea urchin mesenchyme ingression and ingression of cells through the primitive streak of amniotes, but retains the implication that the epithelial cells undergo an epithelial-to-mesenchymal transition at some point during the process.

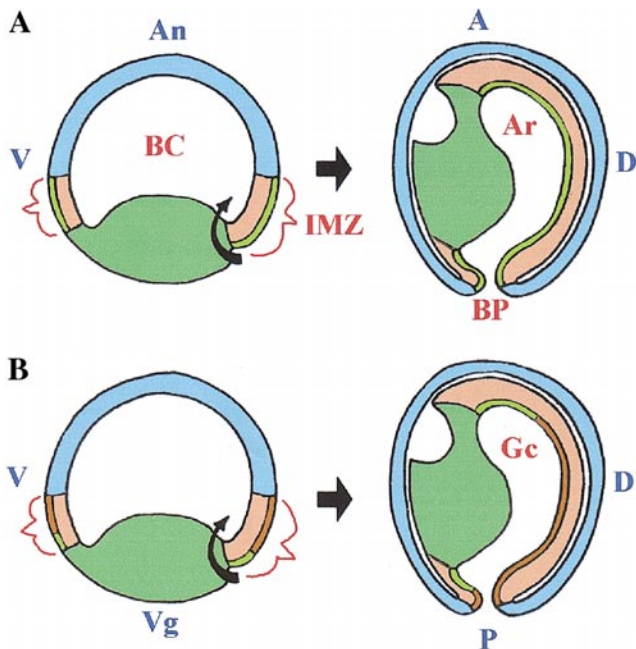


FIG. 1. (A) Diagrams show that involution of the IMZ of a gastrula with presumptive mesoderm only in the deep layer (pink) brings this germ layer in to its definitive position between the ectoderm (blue) and the lining of the archenteron (Ar) or presumptive gut (yellow-green). (B) In contrast, the same morphogenic movement of the IMZ in a gastrula having presumptive mesoderm in the superficial epithelial layer (red) leaves this component of the presumptive mesoderm on the surface of the gastrocoel (Gc), necessitating its removal by an additional morphogenic movement, ingressión. Blue, ectoderm; green, sub-blastoporal endoderm; yellow-green, supra-blastoporal endoderm; pink, deep mesoderm; red, superficial mesoderm. V, ventral; D, dorsal; An, animal; Vg, vegetal; A, anterior; P, posterior.

pearing under the adjacent endoderm were retro-mapped by tracking the cells apparent at the junction of the endoderm and the ingressing tissue in the last frame of movies; in some cases, the cells at the junction were not identifiable, and so the nearest identifiable cell was tracked. These cells were followed through previous frames to the start of the movies. The positions of these cells are indicated in figures. The same approach was used for lateral marginal zone explants, except that cells on the edge of the region of de-epithelialization were retro-mapped.

Surface Biotinylation

The surface layer of cells was labeled with biotin, usually just prior to gastrulation, based on Minsuk and Keller (1996), with some

modifications. The standard culture media for each species was used and pH was adjusted to ~ 7.5 after the addition of biotin (EZ-Link Sulfo-NHS-LC-Biotin; Pierce No. 21335). Biotin was visualized with either alkaline phosphatase-conjugated streptavidin (Vector Labs No. SA-5100) as in Minsuk and Keller (1996) or by using rhodamine-conjugated avidin D (Vector Labs No. A-2002). When the first method was used, heavily pigmented embryos sections were bleached overnight in PBS with 1% H_2O_2 after the color reaction was complete.

For the second method, only albino embryos were used. After fixation, they were rehydrated into PBS + 0.01% Tween 20, fractured in the desired orientation with a No. 15 scalpel blade, and then processed as in Minsuk and Keller (1996) for avidin binding. Embryos were then dehydrated into methanol, and the half-mount prep from Davidson and Keller (1999) was used to view embryos on the confocal fluorescence microscope.

Immunocytochemistry

Embryos or explants were fixed in sialanized vials for 5–10 min at $-20^\circ C$ in Dent's fix, then overnight at $-20^\circ C$ in fresh Dent's fix, then stored in 100% methanol. For staining, samples were gradually rehydrated into PBS, blocked in PBS + 10% goat serum, incubated in 1:500 rabbit anti-cingulin (antibody No. C-532; Cardellini *et al.*, 1996) in PBS + 10% goat serum overnight at $4^\circ C$, washed in PBS, and then reacted with a fluorescent anti-rabbit secondary. Samples were then prepared for confocal fluorescence microscopy.

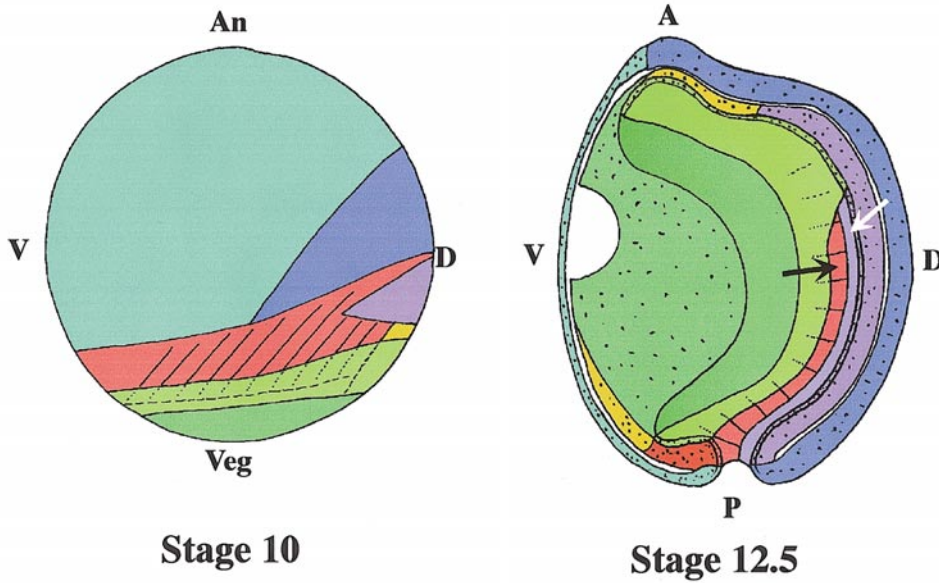
RESULTS

Tracing the Fates of Surface Cells and Apical Cell Surfaces with Biotin Labeling

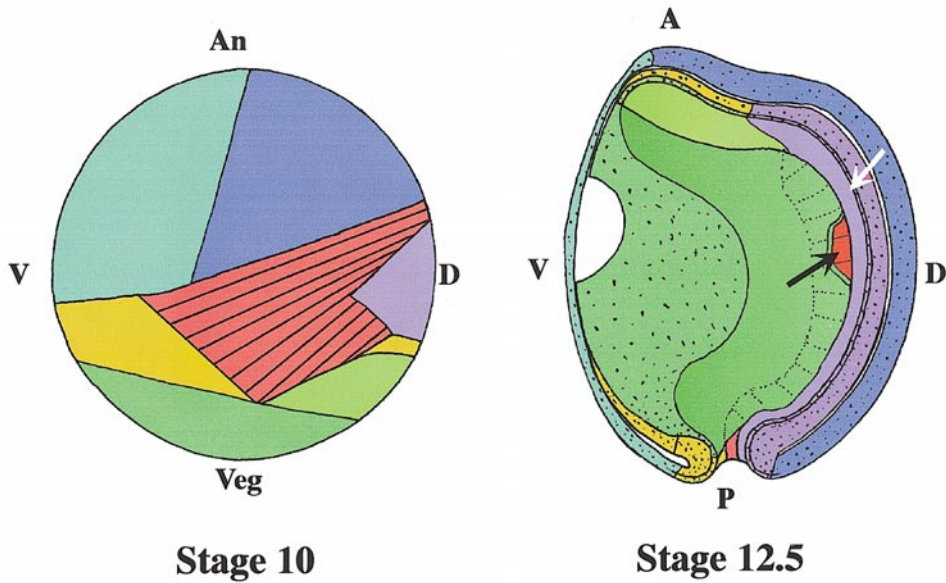
Surface biotinylation marked all the cells that were in the superficial epithelial layer at the time of biotinylation. Biotinylation just prior to the onset of gastrulation specifically labeled the entire surface of the embryo (e.g., Fig. 3A). No surface-labeled cells appear in the deep layer prior to neurulation in anurans (Minsuk and Keller, 1997; Shook and Keller, unpublished data). Only faintly labeled vegetal endodermal cells (also see below) were seen in urodeles prior to midgastrulation (e.g., Fig. 3A and data not shown), at which stage time-lapse movies first showed directly that ingressión began (see below). Some embryos were overstained when reacting alk-phos conjugated avidin with NBT and BCIP, in which case the entire embryo appeared labeled; such embryos were disregarded. Each observation of biotin staining documented here was substantiated by a minimum of five embryos; any cases of variance are noted. Unbiotinylated control embryos never showed any signal with a label-conjugated avidin. Thus, any biotin seen in the

FIG. 2. Diagrams of the early gastrula stage (stage 10) and the late gastrula stage (stage 12.5) show differences between generalized anuran (A) and urodelean (B) gastrulation. Bluish colors represent presumptive ectoderm (light blue, epidermis; dark blue, neural), reddish colors presumptive mesoderm (magenta, notochordal; red, somitic; orange, head; lateral and ventral mesoderm), greenish colors represent endoderm (yellow-green, supra-blastoporal endoderm; lime green, sub-blastoporal endoderm). Dorsal (D), ventral (V), animal (An), vegetal (Veg), anterior (A), and posterior (P) are indicated. The stage 10 fate map shows only the superficial view. In general, the presumptive fates

A **Generalized Anuran**



B ***Ambystoma mexicanum***



continue radially toward the blastocoel, except that the presumptive head mesoderm in both classes of amphibian and the presumptive lateral plate and some of the presumptive somitic mesoderm (dashed lines, A) in anurans continues vegetally under the superficial layer of the supra-blastoporal endoderm. The stage 12.5 fate map shows a sagittal section of an embryo, such that the stippled tissues are at the face of the cut, while the surface of the gastrocoel cavity curves into the page. In the anuran (A), both the notochord (white arrow) and medial somitic tissue (black arrow) remain on the surface of the gastrocoel, the latter flanked by the medially progressing lateral endodermal crests (yellow-green). In *A. mexicanum* (B), the notochord (white arrow) is now flanked by the sub-blastoporal endoderm (lime green), while the somitic tissue (black arrow, cut away, (B)) has disappeared beneath the endoderm. The plug of vegetal endoderm (yolk plug) extending from the gastrocoel floor into the blastopore at stage 12.5 is not shown (schematics based on Vogt, 1929; Pasteels, 1942).

deep layers was assumed to be associated with cells that had ingressed.

Surface biotinylation also showed that the apical membrane of superficial cells was endocytosed as development proceeded, a result of apical membrane recycling that occurs in most cells (reviewed in Mostov *et al.*, 2000). Internalized biotin was especially evident in bottle cells (Fig. 3A, small arrows) and at a lower level in other superficial or superficially derived cells (Figs. 3A–3D). Apical membrane internalization occurred both in bottle cells of the dorsal blastoporal lip (Fig. 3A, small arrows), which will later respread and remain superficial (Vogt, 1929; Pasteels, 1942), and in more lateral bottle cells, which constricted their apices as a prelude to ingression (Fig. 3B). The faintness of label in ingressed deep cells (Figs. 3C and 3D, small arrowheads) suggested that the biotin-labeled cell surface proteins, or the linked biotin, are degraded after endocytosis. A gradual elimination of biotin label with time is also seen in anurans (Shook and Keller, unpublished data), but to a lesser extent. Thus, absence of label does not necessarily preclude a superficial origin, and biotin-labeling data were interpreted in the light of other experimental evidence, such as time-lapse tracing of cells.

Fate of the Superficial Presumptive Mesoderm and the Timing of Its Ingression

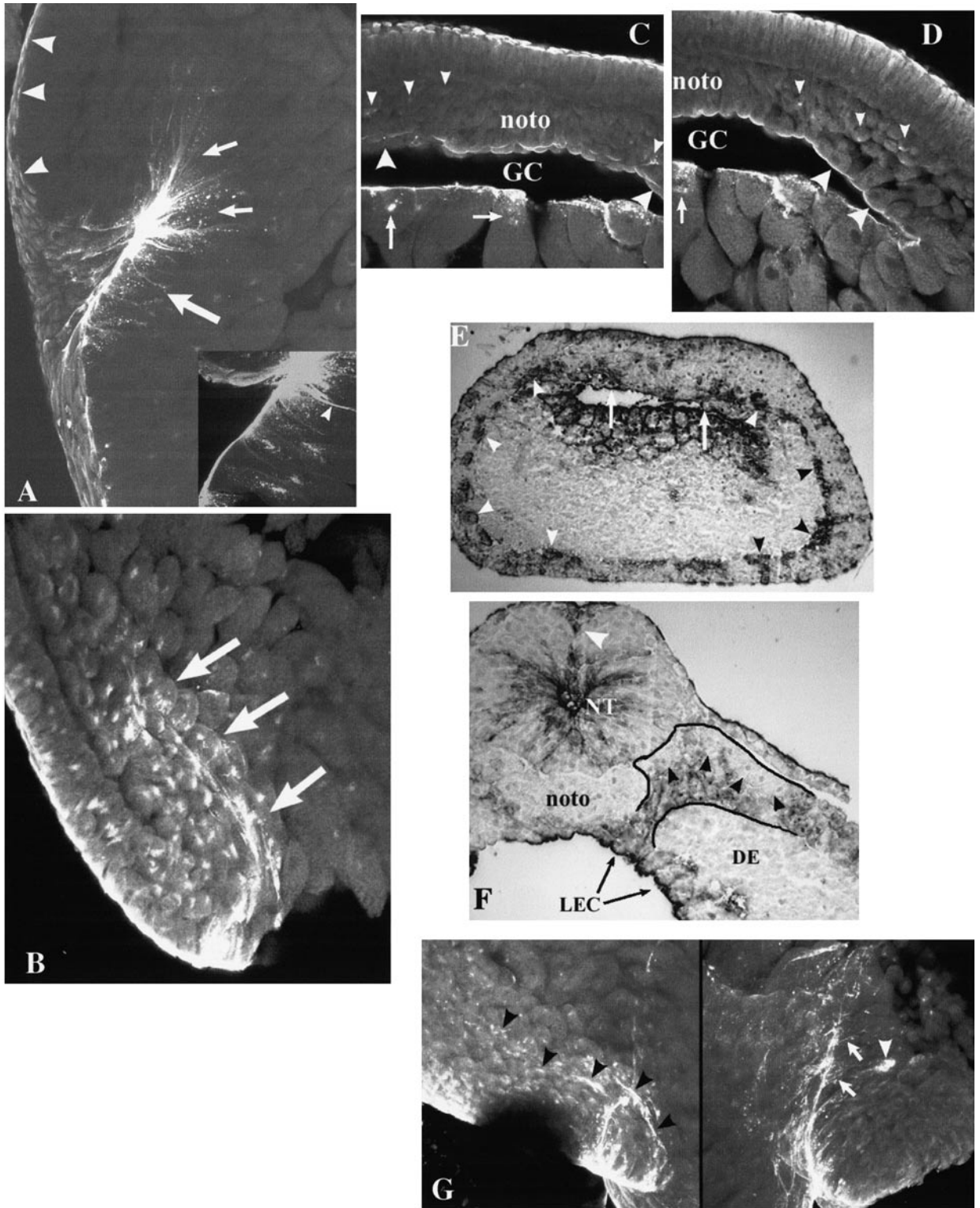
By midgastrulation (stage 11.5), presumptive mesodermal cells had begun ingressing from the surface into the deep layers just inside the lateral blastopore (Fig. 3B, arrows) and are found in the deep somitic mesoderm lateral to the notochord after stage 12.5 (Figs. 3C and 3D, small arrowheads). The cells lining the roof of the gastrocoel appear to be presumptive notochord cells, flanked by larger endodermal cells (Figs. 3C and 3D, large arrowheads). At stage 13.5, biotin-labeled somitic and ventral–lateral mesoderm cells are scattered throughout the circumference of the mesodermal mantle surrounding the endoderm (Fig. 3E, arrowheads), beginning above the medial edge of the lateral endodermal crest (Fig. 3E, arrows) and continuing through

the ventral side. By stage 19, generally all but the dorsal part of the somite is labeled (Fig. 3F, black arrowheads); however, the proportion of the dorsal somite that was unlabeled was variable. The apical face of the notochordal plate, which has not yet ingressed, is labeled, but the deep portion of the notochord is not (Fig. 3F).

Rotations of confocal stacks of the stage 12.5 blastopore region (Fig. 3G; see Fig. S1 at the Web site http://faculty.virginia.edu/shook/uro1/supp_figs.htm) showed the geometry at the site of ingression. The aperture of the gastrocoel spanned only the dorsal quarter of the circumference of the blastopore lip. Just inside the lateral and ventral blastopore lips, presumptive mesodermal cells were ingressing out of the superficial epithelial layer, rather than involuting as an intact epithelial sheet to line the gastrocoel. Biotin-labeled cells were seen in involuted deep tissue lateral to the blastopore (Fig. 3G, arrowheads, especially evident on the left). The lateral limits of the dorsal blastopore that forms the aperture of the gastrocoel are visible as two roughly parallel vertical lines of label (probably representing constricted apices), with that on the right being much stronger. Several bottle cells (Fig. 3G, arrows; see Figs. S1C and S1D at the Web site http://faculty.virginia.edu/shook/uro1/supp_figs.htm) with very elongated necks are attached at the line of label on the right; these probably represent the cells (probably presumptive somitic) seen ingressing along the lateral edge of the posterior notochord in time-lapse recordings (shown below).

In biotinylated embryos of all species we have tested, the deep vegetal endodermal cells under the floor of the gastrocoel were often labeled (e.g., Fig. 3E), but it is not clear whether this represents ingression of surface endodermal cells or biotin endocytosis, followed by radial cleavage. Endoderm cells lying vegetal to the inflection point of the dorsal blastopore early in gastrulation show much internalized label (e.g., Fig. 3A, large arrow). Bottle cell necks full of biotin label (Fig. 3A inset, arrowhead) were sometimes found within this region, and in older gastrulae just vegetal of the inflection point of the lateral blastoporal lip (see Fig. S1D at http://faculty.virginia.edu/shook/uro1/supp_figs.htm).

FIG. 3. Superficially biotinylated *A. mexicanum* (A–D, G) and *A. maculatum* (E, F) embryos show surface-derived cells, visualized with RITC avidin in the first case and with alk-phos avidin in the second case. A projection of a sagittal–parasagittal confocal series of a stage 10⁺ embryo (A) shows that biotin has been internalized in the bottle cells of the dorsal lip (arrows) and in the sub-blastoporal endoderm (large arrow). Only the surface of the marginal zone (arrowheads) is labeled, with no label in the deep cells of this region. A projection of a subset of confocal sections (inset) through the region just vegetal of the blastoporal lip shows internalized biotin, including some in a bottle cell neck (arrow head). A projection of a frontal confocal series through the lateral blastopore of a stage 11.5 embryo (B) shows biotin label in deep mesodermal cells (arrows). A projection of a confocal series through the gastrocoel (GC) of a transversely fractured stage 12.5 embryo (C) shows biotin label in somitic cells (small arrowheads) and just apical to the nuclei of sub-blastoporal endodermal cells (arrows). The large arrowheads show the lateral endodermal crests composed of large endodermal cells flanking the notochord (noto). A single section (D), located just to the right of that shown in (C), shows biotin around the nucleus of a sub-blastoporal endodermal cell in the gastrocoel floor (arrow) and in somitic cells (small arrowheads). Large arrowheads indicate large endodermal cells flanking the notochord. A cross-section of a stage 13.5 embryo (E) shows biotin label scattered throughout the mesodermal mantle (black and white arrowheads) and



in the vegetal endoderm under the gastrocoel floor. The medial extent of the lateral endodermal crests (arrows) are indicated; the right side of the gastrocoel has collapsed. A cross-section of a stage 19 embryo (F) shows superficially derived tissue, including neural tube (NT), possible neural crest (white arrowhead), and notochord (noto). Deep endoderm (DE), unlabeled somitic tissue (black arrowheads), and the limit of the somitic tissue (black lines), and the lateral endodermal crests (LEC) are indicated. Side-by-side projections of a frontal confocal series of a stage 12.5 embryo (G) show label in deep cells (black and white arrowheads) and in necks of bottle cells (arrows). The sections extend roughly from the level of the dorsal blastopore (closest to the viewer) toward the ventral-lateral region of the blastopore.

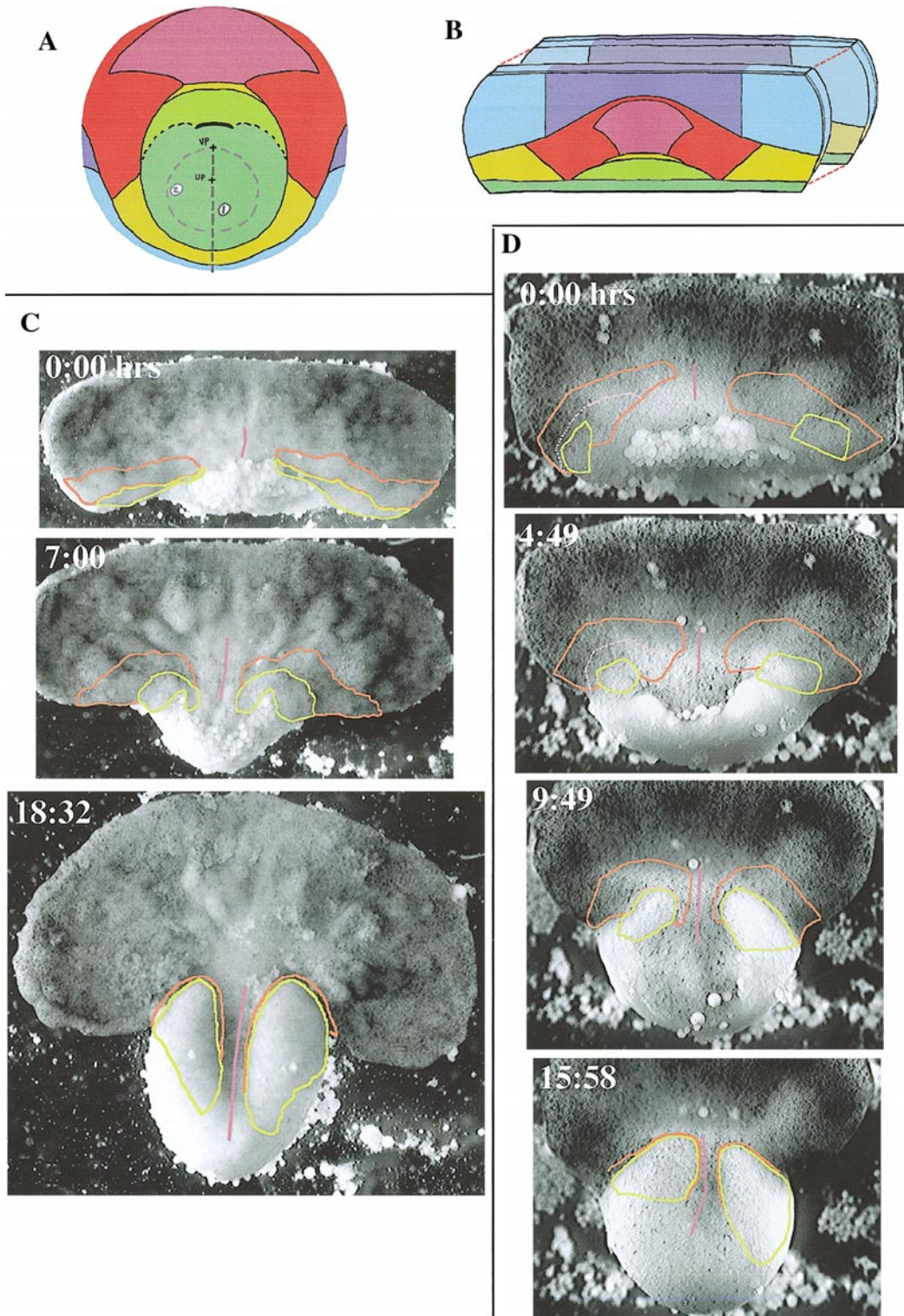


FIG. 4. Diagrams show the construction of a giant sandwich explant. Presumptive germ layers are colored as in Fig. 2. The embryo (A, vegetal view, dorsal above) is cut through the ventral midline (cut #1) and the most vegetal yolk trimmed away (cut #2). The explant is then laid flat and trimmed (B), and two such explants are placed deep sides together and allowed to heal. Frames from a typical time-lapse recording of giant sandwich explants of *A. mexicanum* (C) and *T. granulosa* (D) show subducting cells (orange outlines) disappearing under the endoderm (yellow outlines) and the extension of the notochord (magenta line). Animal is above, vegetal below, dorsal is at the midline of the explants, and ventral is at the lateral edges. The dotted pink line in (D) maps the movements of an intermediate set of subducting cells. Times indicate hours and minutes elapsed from the first frame (about stage 10) to the last (about stage 12.5) (see Figs. S2 and S3 at http://faculty.virginia.edu/shook/uro1/supp_figs.htm).

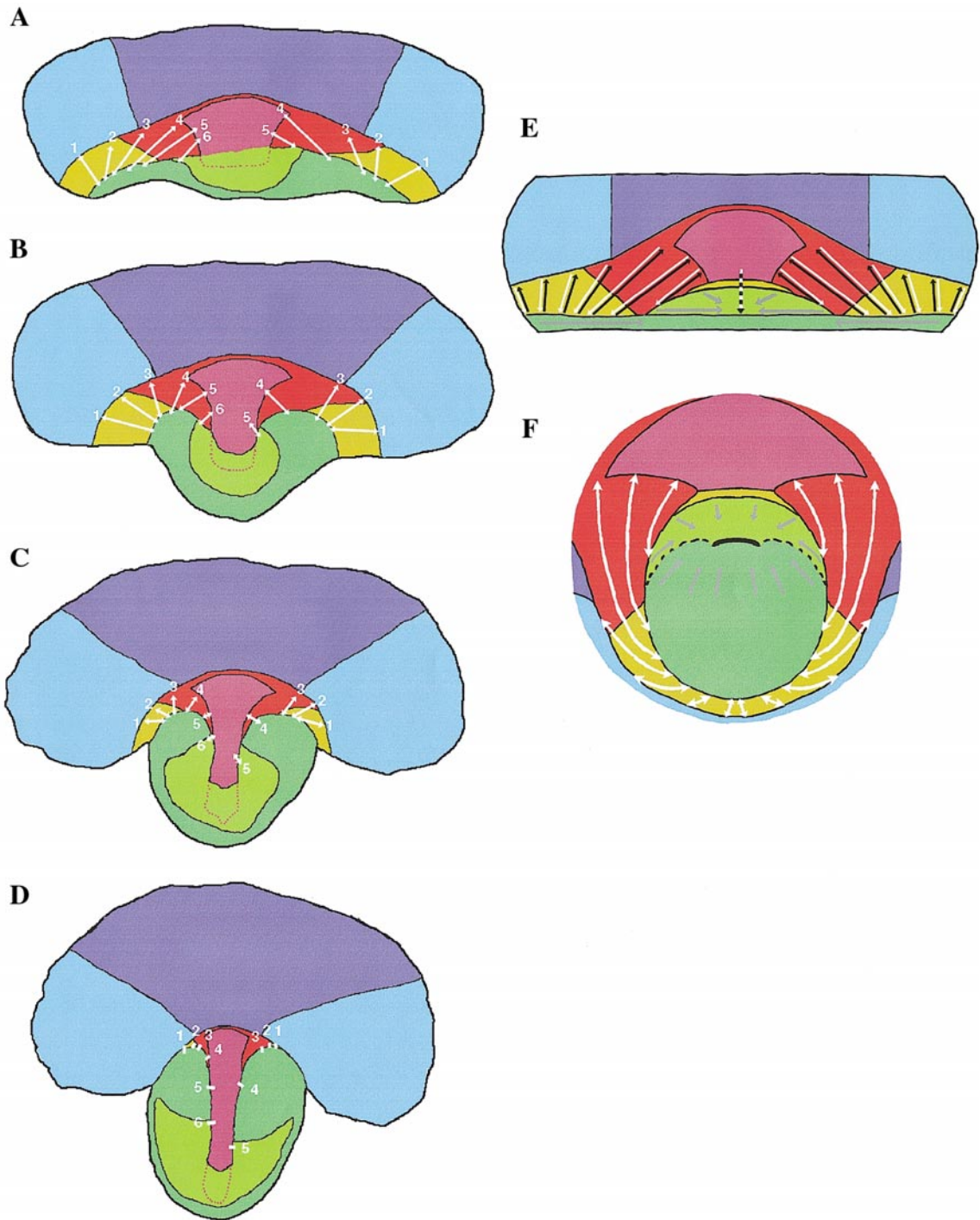


FIG. 5. Diagrams show the subduction movements in recording frames of Fig. 4C: 0:00 (A), 7:00 (B), 12:43 (same explant but not shown in Fig. 4C) (C), and 18:32 (D). A generalized initial explant (E) and a whole embryo (F) are shown. Numbered, double-headed arrows in (A–C) correspond to pairs of cells that come to be adjacent in (D). The dotted purple line in (A–D) estimates the extent of the deep anterior notochord. White arrows in (E) indicate the subduction of the superficial presumptive mesoderm under the endoderm; black arrows indicate the progression of apical constriction behavior within the superficial presumptive mesoderm. Gray arrows in (E) and (F) depict generalized movements due to endodermal bottle cell constriction. White arrows in (F) indicate points in the superficial presumptive endoderm and notochord that will come to lie next to each other due to subduction (as in A–D).

Place, Timing, and Pattern of Superficial Presumptive Somitic Mesoderm Subduction

Biotinylation showed the fate in the deep layers of mesodermal cells that originate superficially but not their specific place of origin or subsequent morphogenesis. Giant sandwich and dorsal isolate explants allow time-lapse recording, with single cell resolution, of superficial presumptive mesodermal cell ingression, inferred from biotinylation studies. Each type of explant has specific advantages that allow us to focus on different aspects of superficial mesoderm morphogenesis.

Gastrulation in a plane: giant sandwich explants.

Giant sandwich explants (Fig. 4) place the embryonic tissues of interest in a single plane, including those around the blastoporal lip where superficial presumptive mesoderm appears to ingress, based on our biotinylation experiments above. Giant sandwich explants were made at stage 10 by cutting two *A. mexicanum* embryos along the ventral midline and removing tissue around the vegetal pole, thus leaving some sub-blastoporal presumptive endoderm below the bottle cells or presumptive bottle cells (Fig. 4A). Deep vegetal endoderm and any involuted cells were removed from the blastocoel walls, taking care to leave the bottle cells intact. The animal edges were trimmed to match one another, and the isolates were then placed with their deep layers facing each other and allowed to heal under a coverslip for 1–4 h, after which the cover slip was removed, and time-lapse recording began (see Fig. S2 at http://faculty.virginia.edu/shook/uro1/supp_figs.htm).

Retro-mapping a representative explant back to the early gastrula stage shows that a large region of the IMZ (Fig. 4C, orange outline), the presumptive somitic and lateroventral mesoderm (Fig. 2B, St. 10), disappeared beneath the animal edge of the presumptive endoderm (Fig. 4, yellow outlines). As this movement appears similar in geometry to one continental plate (the mesoderm) subducting under another (the endoderm), we refer to it as subduction. We call the junction between the two tissues the “subduction zone” (SZ). As gastrulation proceeded, the presumptive notochordal region extended (Fig. 4C, medial magenta line), and both the presumptive somitic and lateral–ventral mesodermal regions (Fig. 4C, orange outlines) and the endodermal regions (Fig. 4C, yellow outlines) converged and rotated their animal edges toward the midline. As the presumptive superficial somitic mesoderm subducted under the endoderm, the endoderm came to lie along side the extending notochord (Fig. 4C), in an anterior-to-posterior progression that corresponds with involution in the whole embryo (Fig. 5).

The presumptive somitic areas began to contract (Fig. 4C, orange outlines) as a result of constriction of individual cell apices. This occurred progressively, beginning in the most medial³–vegetal cells within the presumptive somitic me-

sodermal region at about 3.5 h from the first frame of the movie (between stages 10.5 and 10.75) and then sweeping laterally along the vegetal edge of the presumptive lateral plate mesoderm (see Fig. 2B, Stage 10⁻). Apical constriction over this broader region began at about 4.5–5 h, as control embryos were approaching midgastrula stage (stage 10.75) and the lateral–ventral blastopore was forming. This initial group of cells constricting their apices along the vegetal edge of the marginal zone corresponded to the cells that would initially form the lateral and ventral blastopore in the intact embryo. This initial contraction of the lateral ventral bottle cells also caused the vegetal edge of the explant to contract toward the midline (Fig. 4C, 0:00–7:00 h).

Subduction began in explants when the ventral blastopore was complete (stage 11) in whole embryos. Beginning at about 7 h, just past control stage 11, presumptive mesodermal cells adjacent to the presumptive endoderm ingressed directly into the deep layer as their apices contracted. A distinct boundary soon formed between the mesoderm and endoderm, and directed movement of the former under the latter was apparent by 8.5 h, when controls were approaching late gastrula stage (stage 11.5). Subduction continued in these explants, with an attendant expansion and extension of the endoderm in the anterior–posterior axis (Figs. 4C, 18:32), until control embryos were at late gastrula stage (stage 12.5). Subduction continued beyond the late gastrula and into the early neurula in what would, in an intact embryo, be the region just inside the lateral and ventral blastopore. However, we could follow it more reliably in the dorsal isolates made at the late gastrula stage (see below).

Of other *A. mexicanum* giant sandwich explants constructed as above and that had clear views of the subduction zone, similar subduction movements were observed in six of six explants. In two other explants, the sub-blastoporal endoderm was seriously damaged in the process of explant construction and no longer had an epithelial connection to the adjacent prospective mesoderm; in these cases, cells constricted their apices and moved through what would have been the subduction zone, but instead appeared to de-epithelialize. In two other explants that remained under coverslips for >15 h, strong subduction movements were not obvious. And in one explant that did not contain sub-blastoporal endoderm, strong subduction movements were again not obvious. The geometry and time course of subduction movements in two of two giant sandwich explants made from *A. maculatum* embryos were similar (not shown). Subduction movements are summarized schematically in Fig. 5.

Results from *Ambystoma* suggested that subduction might be a general feature of urodele gastrulation, in con-

³ We use the terms “medial,” “lateral,” “dorsal,” and “ventral” here to indicate the position of tissues as they lie in the gastrula-stage embryo, with respect to the dorsal midline of the notochord or the dorsal blastopore lip. They should not be taken as indications

of the eventual, postgastrulation orientation of these tissues, which may be different, although apparently less so for the *urodeles* (see Fig. 2) than for *Xenopus* (Keller, 1992).

trast to anuran gastrulation. We tested this hypothesis by examining *T. granulosa*, a species from a different urodele family but within the same suborder (Salamandroidea). Seven of seven giant sandwich explants of *T. granulosa* made as detailed above showed the same subduction behavior as *A. mexicanum* and *A. maculatum* (e.g., Fig. 4D; see Fig. S3 at http://faculty.virginia.edu/shook/uro1/supp_figs.htm), suggesting that subduction and this style of gastrulation are common to an entire suborder of, if not all, urodeles. The primary differences between the two groups are that *T. granulosa* shows little expansion of the ectodermal area and it shows less notochordal extension during gastrulation (compare Figs. 4C and 4D). When mesodermal subduction is retro-mapped from a middle time point, the majority of the initial subduction was of the most medial-vegetal tissue (Fig. 4D, 0:00–9:49, dotted pink line), demonstrating that in this species subduction also progresses laterally around the blastopore and then anteriorly.

Summary of the geometry of subduction. We mapped the subduction movements seen in the giant sandwich explant (Fig. 4C) back onto the initial fate map to understand better the geometry of subduction. We matched adjacent cells in the superficial presumptive mesoderm and endoderm at the end of the movie (Fig. 4C, 18:32) and retro-mapped these pairs back to the first frame (Figs. 5A–5D, arrows). We then generalized these movements onto the fate map of the initial explant and the intact embryo (Figs. 5E and 5F). Three sets of movements collaborate to drive the observed morphogenesis. First, bottle cell contraction along the blastopore draws the vegetal edge of the marginal zone toward the dorsal midline (Fig. 5E, gray arrows). Second, involution, coupled with the convergence and extension of the midline tissues and the re-expansion of the supra-blastoporal endoderm draws cells into the embryo and extends them anteriorly (Fig. 5E, striped arrow). Third, the progressive vegetal-to-animal apical constriction of the superficial presumptive somitic and lateral-ventral mesodermal cells (Fig. 5E, black arrows), coupled with their progressive subduction under the endoderm (Fig. 5E, white arrows), draws the sub-blastoporal endoderm toward the lateral edge of the notochord, or in the case of the most ventral sub-blastoporal endoderm, toward the ectoderm (Fig. 5E, black arrows).

Gastrulation from the inside: dorsal isolates. Dorsal isolates (Fig. 6) allow recording of the SZ in the normal tissue geometry and with involution, thus revealing any abnormalities caused by the planar array of tissues and the prevention of their involution in giant sandwich explants.

Late gastrula stage (stage 12–12.5) embryos were cut along the ventral midline, through the yolk plug and the floor of the gastrocoel, and gently teased open to avoid tearing the blastoporal region. About a quarter of the anterior gastrocoel roof was trimmed off (to avoid its interference with observation) and much of the ventral tissues, including most of the ventral vegetal endoderm, was trimmed away, but leaving most of the epithelial lining of the gastrocoel intact. The explants were then cultured with the gastrocoel roof up and held open by light pressure from a coverslip, or cultured with the roof down and held open by their own weight. The explants were allowed to heal for 30 min to 1 h and then turned roof up, or in the case of those isolated with the roof up, the coverslip was removed before time-lapse recording. Dorsal isolates were sometimes cultured in flat, shallow wells melted into agarose to prevent migration of the explant during time-lapse imaging.

Dorsal isolate explants of *A. maculatum* revealed the movements of the tissues of the gastrocoel roof and the inner blastoporal lip (Fig. 6). Time-lapse recordings of these explants began during late gastrulation, at about the same stage (12.5) that the example shown for the giant sandwich explants ended. By this time, the surface layer of the presumptive notochord had already involuted, converged, and extended, but remained on the surface to form the notochordal plate (cf. Fig. 2B). In dorsal isolate explants, only a few cells ingressed at the lateral edge of the extended notochordal plate prior to the ingression of the notochordal plate itself around the time of neural tube closure. For example, four cells with constricting apices appeared to be withdrawing from the side of the posterior notochordal plate, anterior of the blastoporal region (Fig. 6, fat red arrowheads). As involution and extension carried the notochordal plate anteriorly, the two cells at the bottom of the frame ingressed, while the two at the top of the frame remained on the surface but showed very small apices by late neurula stage (Fig. 6, 9:20; see Fig. S4 at http://faculty.virginia.edu/shook/uro1/supp_figs.htm). This small amount of ingression occurring on both sides of the superficial notochord represents the completion, during neurulation, of the ingression of the medial edge of superficial presumptive somitic cells, which began as subduction, described in the giant sandwich explants above.

In contrast to the sparse ingression seen along the notochordal plate just anterior of the blastoporal region, a great many cells leave the surface layer from two posterior bilateral regions, flanking the presumptive notochord, just inside the lateral and ventral blastopore during neurula-

FIG. 6. Diagrams show the construction of a dorsal isolate explant (A). The gastrocoel roof is explanted by cutting through the ventral midline at stage 12 (cut #1), spreading the embryo open on its dorsal surface, and trimming off most of the vegetal endoderm (cut #2), and trimming off the anterior gastrocoel. The gastrocoel roof surface is imaged and recorded, either with (shown) or without a restraining coverslip (c.s.). Dorsal (D), ventral (V), notochord (N), endoderm (E), and somitic mesoderm (S) are indicated. Frames from a typical time-lapse recording (B) of an *A. maculatum* explant shows extension of the notochord (black arrows) and movements of subducting cells just inside the blastopore (dotted orange line) toward the subduction zone (yellow/orange double line). White arrows indicate cells traced

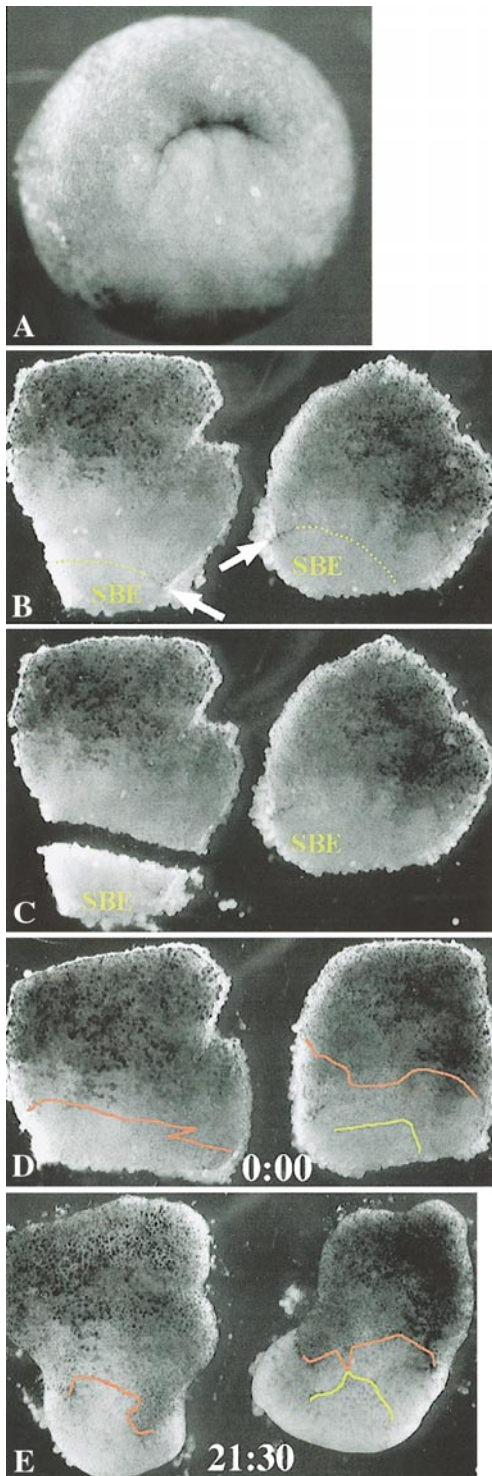


FIG. 7. Lateral marginal zone explants of roughly 90° were made from the left and right sides of a stage 10.5 *A. mexicanum* embryo (A), and the sub-blastoporal endoderm (SBE) was trimmed from one of them (left one; B, C) well above the forming bottle cells (B, arrows) and imaged in time-lapse recordings (D, E). The orange line represents the upper limit of de-epithelialization in the mesoderm,

tion (Fig. 6B, areas outlined in orange in blastoporal area, right; see Fig. S4 at http://faculty.virginia.edu/shook/uro1/supp_figs.htm). These regions are the same regions of subduction seen late in recordings of giant sandwiches at the posterior end of the extending axis (see also Fig. 5). Cells roll around (involute over) the blastopore lip of the dorsal isolate and then subduct under the endoderm (Fig. 6B, Endo). This SZ is indicated by the adjacent yellow and orange lines between the endoderm and subducting mesoderm (Fig. 6B, 0:00).

Cell behavior prior to subduction varied. The apices of cells within the SZ ranged from highly constricted to those with relatively unconstricted apices (see Fig. S4 at http://faculty.virginia.edu/shook/uro1/supp_figs.htm). Cells began to constrict their apices, apparently somewhat stochastically, generally beginning about 250 μm from the SZ, and with increased frequency as they approached the SZ, such that cells with both small and large apices subduct together. A few cells appeared to ingress prior to reaching the SZ; one cell began contracting its apex while about 190 μm from the SZ, at 2:00 h, and was no longer visible by 4:40 h, while still $\sim 70 \mu\text{m}$ from the SZ (Fig. 6B, thin red arrow head), about 2 h before its neighbors ingressed through the SZ.

Fifteen of fifteen other *A. maculatum* dorsal isolate explants, made as detailed above, that had clear views of the subduction zone showed similar subduction movements. Two explants constructed later than stage 14 did not show obvious subduction movements. In 12 of 12 explants constructed as above that had clear views of the region at the lateral edge of the involuted superficial presumptive notochord, a few cells were observed showing strong apical constriction, and in some cases ingressing. These para-notochordal cell behaviors were observed primarily at earlier stages (e.g., prior to control stage 14), and more often in the posterior gastrocoel roof.

Five of eight *A. mexicanum* dorsal isolate explants showed similar subduction movements (data not shown). In the three remaining explants, the endodermal epithelial layer ripped away from the underlying mesenchymal cells near the blastopore during explant construction, making the details of subduction hard to observe. However, in at least one of these cases, the absence of the endodermal epithelium clearly revealed the transition of the mesodermal cells from an epithelial cell type with generally constricted apices to a mesenchymal cell type, as they pass through what would be the SZ.

while the yellow line represents the lower limit of de-epithelialization in the sub-blastoporal endoderm. (see also Fig. S5 at http://faculty.virginia.edu/shook/uro1/supp_figs.htm).

Correspondence of Subduction Movements between Explants

The movements of the subducting cells were very similar in the giant sandwich and dorsal isolate explants, and appeared to reflect the mechanics of subduction and involution found in the whole embryo. Using Object Image, we found that superficial mesodermal cells pass through the zone $\sim 250\text{--}100\ \mu\text{m}$ from the SZ at about the same average rate ($43\ \mu\text{m}/\text{h}$ in giants and about $40\ \mu\text{m}/\text{h}$ in dorsal isolates). The pattern of movements was also similar. In dorsal isolate explants, individual superficial presumptive mesodermal cells (Fig. 6B, white arrows) were tracked through the blastoporal region and into the SZ; the most medial cells, nearest the SZ, approached the endoderm directly, while the more lateral cells (initially just inside the blastopore lip) first moved medially as they finished involuting, then moved directly toward the endoderm (see Fig. S4 at http://faculty.virginia.edu/shook/uro1/supp_figs.htm). By 6 h (Fig. 6B, 6:00), all four cells were adjacent to the SZ, and by 1.5 h later, the posterior vegetal endoderm had spread posteriorly and covered the subducting mesodermal cells. In giant sandwich explants, cells lying in a position equivalent to that of the cells in the lateral portion of the subducting region in the dorsal isolate explant were initially drawn directly toward the SZ, reflecting the contraction of the intervening cell apices. The cells then moved medially for a time, roughly parallel to the SZ, then finally approached the SZ directly (data not shown). This medial movement of the subducting cells, seen in both dorsal isolate and giant explants in a region equivalent to the immediate inside of the blastopore lip in a whole embryo, may correspond to the strong convergence that is coupled with involution around the blastopore lip in whole *Xenopus* embryos (Keller *et al.*, 1992; Shih and Keller, 1992).

Cell Behavior Prior to Subduction

The approach of cells toward the SZ appears to be driven primarily by the apical contraction of cells about $250\text{--}100\ \mu\text{m}$ from the SZ, and thereafter by the spreading of the endoderm over the superficial presumptive mesodermal cells in the SZ. In the dorsal isolate, the frequency of apical constriction increased when cells moved within about $250\ \mu\text{m}$ of the SZ, shortly after involution, although a few began constricting earlier. Cells measured just inside $250\ \mu\text{m}$ from the subduction zone showed an average decrease in surface area of about 50% by the time they came in contact with the endoderm. The rate of approach toward the endoderm due to constriction alone started at $0\ \mu\text{m}/\text{h}$ at $\sim 300\ \mu\text{m}$ from the endoderm and rose to $\sim 30\ \mu\text{m}/\text{h}$ at $125\ \mu\text{m}$.

Within the last $\sim 100\ \mu\text{m}$, movement of superficial presumptive mesoderm cells toward the SZ appeared to be due primarily to endodermal spreading over the mesoderm, rather than mesodermal constriction. Some cells within $100\ \mu\text{m}$ continued constricting as they approached the endoderm, but this accounted for little of remaining ap-

proach. The endoderm adjacent to the SZ spread posteriorly, covering the paraxial mesoderm at $\sim 20\ \mu\text{m}/\text{h}$. It is not clear whether this was the result of active, autonomous endodermal spreading over the constricted mesodermal cells or of active ingression of mesoderm cells pulling the endoderm toward the remaining superficial mesoderm cells, or both. Mesodermal cells took an average of 20–38 min to subduct under the endoderm after coming into contact with it. In some movies of the SZ in dorsal isolate explants, the apical surface of the endodermal cells appeared to extend protrusions onto the surfaces of the subducting mesoderm, but it is extremely difficult to view the SZ at high enough resolution to confirm these observations. Such protrusions could reflect an active traction of the endoderm cells on the apical surfaces of the mesodermal cells. These protrusions were not observed in giant sandwich explants, and so may be restricted to the normal geometry of the SZ at the base of the blastoporal cleft.

Lateral Marginal Zone (LMZ) Explants Showing De-epithelialization and Subduction Are Progressive and Independent of One Another and Independent of the Endoderm/Blastoporal Region

Lateral marginal zone (LMZ) explants were compressed under a coverslip such that the cells were allowed to undergo apical constriction but could not move into the deep region or otherwise crawl away because of mechanical constraint. LMZ explants consisting of a lateral 60° sector of the embryo, including the lateral tip of the blastopore lip (Fig. 7B, arrows) and much of the vegetal endodermal epithelium, were made from stage 10.5^+ (blastopore $\sim 1/3$ complete) *A. mexicanum* embryos. Two LMZ explants were made from the same embryo (Fig. 7), and the presumptive blastoporal bottle cells and sub-blastoporal endoderm were removed from one of the explants (Fig. 7C, left). The explants were then pressed tightly under a coverslip, thus keeping all the surface cells in a single plane such that there was no place into which they could ingress.

Time-lapse recordings of LMZ explants showed a wave of apical constriction, followed by a wave of de-epithelialization and mesenchyme-like deep cell motility. Apical constriction began at the dorsal, vegetal edge of the explant and very rapidly spread laterally and ventrally. From this vegetal origin, it spread animally. De-epithelialization followed the pattern of apical constriction, progressing from vegetal-to-animal at rates of $35\text{--}55\ \mu\text{m}/\text{h}$ once it began (data not shown), similar to the rate at which subducting mesoderm approaches the endoderm bounding the SZ (see above). As apical constriction occurred, cells were pulled toward the region of constriction. The cells at these foci of constriction eventually released their apical junctions and became mesenchymal; in Figs. 7D and 7E, the region below the orange line of the left explant and between the orange and yellow lines in the right explant de-epithelialized. De-epithelialization generally began as cells both at the

edges, and especially in wider explants, in the center of the explant lost their epithelial connections (see Fig. S5A at http://faculty.virginia.edu/shook/uro1/supp_figs.htm). De-epithelialized cells showed the much greater protrusive activity characteristic of mesenchymal cells (see Figs. S5C and S5D at http://faculty.virginia.edu/shook/uro1/supp_figs.htm).

Retro-mapping the de-epithelialized regions to the first frame showed that some but not all of the mesoderm that would subduct in a giant sandwich explant de-epithelialized in these explants. However, more mesoderm de-epithelialized in the explant without blastoporal bottle cells or sub-blastoporal endoderm (Figs. 7C–7E). Apical constriction and de-epithelialization of the superficial presumptive mesodermal cells during subduction did not depend on their actual ingression. It also did not depend on initiation by the blastoporal bottle cells or on continuous contact with the sub-blastoporal endoderm, nor did it require a free epithelial edge in the region that de-epithelialized.

De-epithelialization is not simply a result of pressing an epithelial tissue under a coverslip but is specific to the somitic and lateroventral mesoderm. Five of five animal cap explants showed no significant de-epithelialization (data not shown), nor did the sub-blastoporal endoderm (e.g., Fig. 7, right side, below yellow line) under the same conditions. Dorsal marginal zone explants otherwise constructed as for LMZ explants show de-epithelialization only in lateral regions fated to become somitic mesoderm. The presumptive notochord remains epithelial until much later, when it too begins to de-epithelialize (see Fig. S5B at http://faculty.virginia.edu/shook/uro1/supp_figs.htm), reflecting its normal late ingression.

De-epithelialization in LMZ explants is typically delayed, however, compared with subduction in giant sandwich explants. Cells began to constrict apically at a similar time and in a similar spatial progression in LMZ explants but did not begin to de-epithelialize until about 7 h (stage 11.5⁺), almost 2 h after subduction became obvious in giant sandwich explants. De-epithelialization did not become widespread until about control stage 12, 5 h later.

Similar de-epithelialization behavior was seen in 26 of the 32 LMZ explants we constructed from *A. mexicanum*; in the 6 remaining cases, subduction rather than epithelialization was observed; this seemed to be correlated with a failure to press the coverslip onto the explant tightly enough. Another 3 explants were discounted, as it was not clear that the presumptive mesodermal epithelium was intact when the explant was made. Three of four LMZ explants made from *A. maculatum* also showed de-epithelialization, while the fourth was ambiguous.

Subducting Cells Do Not Initially Contact the Blastocoel Roof

Ingressing cells do not have immediate access to the blastocoel roof as a substrate upon which to migrate. We

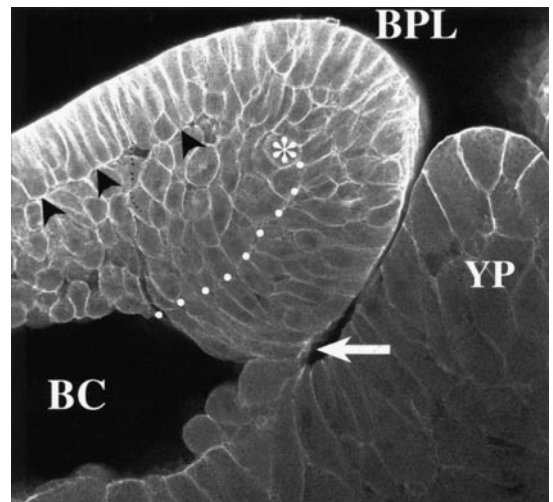


FIG. 8. A confocal image shows β -catenin staining of the lateral blastoporal lip of a stage 13.5 *A. mexicanum* embryo. Cells are ingressing from the left side of the base of the blastoporal cleft (arrow). The more intense staining in the outer portion of the embryo is an artifact of fixation. The approximate location of the inner lip of the blastopore is marked by an asterisk and the approximate extent of ingressing cells still attached to the epithelial layer is indicated by the dotted white line. BPL, lateral blastoporal lip; YP, yolk plug; BC, blastocoel remnant.

stained embryos for β -catenin, a cytoplasmic component of cadherin-mediated intercellular junctions, including adherens junctions, that nicely traces the basal-lateral membrane domains of epithelial cells, presumably localized there by association with cadherins (e.g., Miranda *et al.*, 2001). Ingressing cells (Fig. 8, those just inside the blastopore lip, to the left and down from the dotted white line) were separated from the former blastocoel roof (Fig. 8, arrowheads) by a collar of cells composed of recently involuted deep cells and previously ingressed superficial cells (Fig. 8, those above and to the right of the dotted white line, up to the blastocoel roof). We were unable to resolve whether cells about to ingress have amounts of β -catenin at their apical membrane domains different from cells not fated for ingression.

Epithelial Junctional Remodeling in Subducting Cells

Subduction involves transformation of superficial epithelial cells into deep, nonepithelial (mesenchymal) cells. Thus, it is important to know when and where cells remodel their epithelial junctions, especially in regard to the time of subduction. Antibody staining for cingulin, a cytoplasmic component of tight junctions (Cardellini *et al.*, 1996; Fesenko *et al.*, 2000), outlines the apical surfaces of all the epithelial cells in and around the blastopore (Fig. 9A; to visualize, see rotations of these confocal projections: Fig.

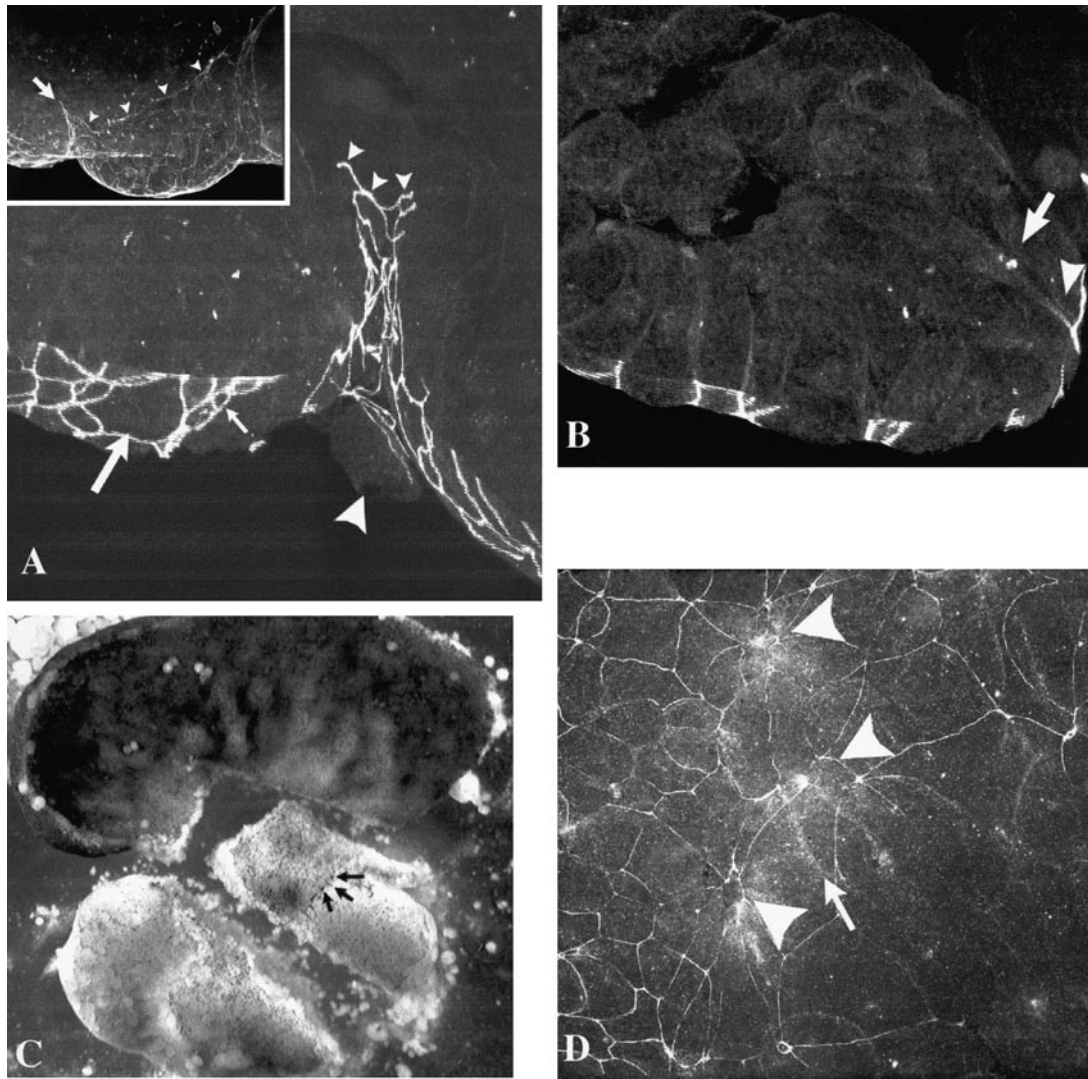


FIG. 9. Confocal sections show cingulin expression in *A. mexicanum*. A projection of frontal sections through the blastopore of a stage 12 embryo (A) shows continuous, intense staining of the periphery of epithelial cells down to the base of the blastoporal cleft (small arrowheads). A large apical cell surface in the marginal zone (large arrow), a small apical cell surface in the marginal zone (small arrow), and a broken fragment of the embryo (large arrow) in the marginal zone are indicated. The inset is a low-magnification view of the blastopore showing the limit of cingulin expression around the blastopore (arrowheads) with the arrow showing the base of the blastoporal cleft seen in the high magnification view. (B) A projection of a subset of slices of the region just left of the blastoporal cleft in (A) shows cingulin labeling in the neck of a bottle cell (arrowhead) and at the apex of an ingressed, bottle-shaped cell. (See also Fig. S6 at http://www.people.virginia.edu/~drs6j/urol/supp_figs.) (C, D) Cells caught in the act of subducting in a giant sandwich explant. (C) The region of interest cut out of the explant (see Fig. S7A at http://www.people.virginia.edu/~drs6j/urol/supp_figs); regions of intense pigmentation where subduction is beginning are indicated (arrows). (D) A projection of an en-face confocal series of the mesoderm/endoderm interface. Arrowheads indicate regions of intense cingulin staining in the subduction zone, and these correlate with the heavily pigmented cell apices indicated in (C). Cingulin expression is shown trailing down the necks of cells with highly constricted apices (e.g., arrow). Rotate projections in the Web site to visualize the cingulin trails (see Fig. S7B at http://www.people.virginia.edu/~drs6j/urol/supp_figs).

S6 at http://faculty.virginia.edu/shook/urol1/supp_figs.htm. There appears to be as much cingulin, and by inference, intact tight junctions (Citi, 1992), per unit circumference in cells about to subduct, right up to the bottom of the blastoporal cleft (Fig. 9A, arrowheads), as in any other

epithelial cell in the embryo. Moreover, circumapical cingulin staining does not vary in intensity with respect to extent of apical constriction of the cells approaching the blastopore and the base of the cleft (Fig. 9A, small and large

arrows; Fig. 9B; see Fig. S6 at http://faculty.virginia.edu/shook/uro1/supp_figs.htm), again showing that the onset of apical constriction appears somewhat stochastic, increasing with frequency as cells approach the SZ. There is diffuse cingulin expression in the deep layers, somewhat concentrated in or around cell nuclei and along cell membranes, and more strongly along the necks of bottle cells (e.g., Fig. 9B, arrowhead); there is also occasional punctate staining in the deep layers (e.g., Fig. 9B, arrow), which is strongest in the yolk plug (Fig. 9A, inset), and at least sometimes appears to be associated with the remaining apical domain of recently ingressed cells (see also Figs S6A–S6D at http://faculty.virginia.edu/shook/uro1/supp_figs.htm).

Ingressing cells can be identified in projections of confocal sections through the SZ in giant sandwich explants. Regions of dense cingulin expression in the SZ of a giant sandwich explant (Fig. 9D, arrowheads) correspond to the dark spots indicating the constricted apices of bottle cells that are about to ingress (Fig. 9C, arrows; see also movie of the giant sandwich explant just prior to dissection: Fig. S7A at http://faculty.virginia.edu/shook/uro1/supp_figs.htm). Rotations of confocal stack projections allow visualization of the streaks of cingulin running from these constricted apices into the subepithelial portion of the explant (e.g., Fig. 9D, arrow; see also Fig. S7B at http://faculty.virginia.edu/shook/uro1/supp_figs.htm).

DISCUSSION

Fate maps of the urodeles *Triturus alpestris* (Vogt, 1929) and *A. mexicanum* (Pasteels, 1942) showed that large areas of presumptive mesoderm in the surface layer of the blastula and that much of the somitic and lateroventral mesoderm leaves the surface layer shortly after involution. But the timing and mechanism of its removal and how such removal functions in gastrulation remained largely a mystery. Here, we show that a massive, specialized, and highly organized form of ingression, termed subduction, removes presumptive somitic and lateroventral mesoderm from the surface layer during gastrulation and neurulation.

We now discuss the implications of our findings in terms of cellular and tissue mechanisms of gastrulation and their evolution, both within amphibians and throughout vertebrates.

The Nature and Function of Subduction of Superficial Mesoderm in Gastrulation

Our time-lapse recordings confirm the results of our biotin-labeling experiments and show directly that the superficial presumptive somitic and lateroventral mesoderm in the pregastrular fate map of *A. maculatum*, *A. mexicanum*, and *T. granulosa* move into the deep layers by subduction, just inside the blastopore. This resolves directly the question of how the notochord comes to be flanked by sub-blastoporal endoderm in the gastrocoel roof

of the embryo (Fig. 2B) (see Vogt, 1929) in representatives of both salamanders (Ambystomatidae) and newts (Salamandridae). We hypothesize that blastoporal subduction is a primitive character of urodeles, and plan to test this by examining representatives of more divergent urodele families.

Subduction consists of an organized, spatially and temporally progressive ingression of cells that begins at the midgastrula stage (stage 11–11.5), and was described previously as “bottle cell ingression” (Vogt, 1929; Holtfreter, 1944; Lewis, 1948, 1952; Lundmark, 1986). Subduction removes nearly all of the superficial somitic and lateral-ventral mesoderm from the surface immediately after involution through the blastopore such that only a few somitic cells are removed from the gastrocoel roof during neurulation. However, subduction of posterior mesoderm just inside the lateral-ventral blastoporal lip continues throughout neurulation and perhaps into tail bud stages.

Subduction begins with the apical constriction of the most medial, vegetal superficial presumptive somitic cells of the gastrula (the future lateral edge of the anterior somitic cells). Apical constriction then rapidly spreads laterally and ventrally around the blastopore, as it continues to form. Apical constriction of cells approaching, and ingression of cells adjacent to, the endoderm–mesoderm junction (the SZ) draws more distant cells toward the SZ. As the initial, most vegetal group of cells begin to subduct, apical constriction spreads to the cells being pulled toward the SZ. The endoderm bounding the SZ may also actively spread over the apical surface of the ingressing superficial presumptive mesodermal cells. Combined, these processes pull cells into the SZ, which remains just inside the blastopore lip, and as superficial cells continue to involute around the blastopore lip, they are absorbed into the deep region by subduction at the SZ. Cells stochastically constrict their apices with increasing frequency as they approach and involute around the blastopore, such that both the breadth and width of the subducting mass of cells decreases as it involutes. Thus, one epithelial sheet appears to slide under another with the ingressing cells becoming mesenchymal as they move into the deep layers. Formally, the EMT occurs when the superficial cells lose their junctional connections with the other superficial epithelial cells, but the steps in this process, and how the epithelium retains its integrity during the process, remain unknown.

A Bilateral Primitive Streak Absorbs the Large Area of Superficial Presumptive Mesoderm during Gastrulation

The apical constriction of a very large area of superficial presumptive mesodermal cells and their subsequent removal from the epithelial layer by subduction just inside the lip of the blastopore has profound implications for the nature of the gastrulation mechanisms and the meaning of the “blastopore” in urodeles. Our results here and our

unpublished data show a major difference between urodeles and anurans in the nature of the blastopore and the behavior of cells around it. In the anuran *Xenopus laevis*, the IMZ is rather thick and relatively small in surface area, with most of the presumptive mesoderm in the deep layers from the onset of gastrulation (Keller, 1991). The little superficial mesoderm that exists in *X. laevis*, both notochordal and somitic, ingresses from the extended roof of the gastrocoel during neurulation (Shook and Keller, unpublished data).

In contrast, the IMZs of the urodeles described here have a large surface area, most of it covered by superficial presumptive mesoderm (see Fig. 2B). But aside from the presumptive notochord, the large area of superficial IMZ involuting over the blastoporal lip never lines the gastrocoel but instead is subducted, or removed from the surface layer, just inside the lip. These differences imply dramatic differences in the mechanisms driving involution and blastopore closure in anurans and urodeles.

Thus, the lateral and ventral blastoporal lips are the bilateral equivalents of the primitive streak of amniotes, based on a number of criteria: (1) a large amount of epithelial tissue is removed from the superficial layer and added to the deep layer in both; (2) both are sites of a massive and progressive EMT; (3) a large amount of cell movement occurs toward a relatively static zone, the internal blastoporal lip in urodeles, the primitive streak in amniotes. The urodele primitive streaks differs from the amniote version primarily by the presence of the vegetal (sub-blastoporal) endoderm separating the paired subduction zones.

This vegetal endoderm remains epithelial in the urodele and is covered over by the IMZ during gastrulation. Its edges are brought in contact with the notochord by subduction of the presumptive somitic and lateroventral mesoderm. Its edges are eventually united mid-dorsally with the ingression of the superficial component of the notochord in the neurula stages, to form the definitive lining of the archenteron. In contrast, the presumptive endoderm of the chick and mouse ingresses and de-epithelializes through the primitive streak, before the mesoderm undergoes these movements, and it apparently re-epithelializes at a later stage, forming the epithelial lining of the archenteron (see references in Bellairs, 1986; Lawson *et al.*, 1991; Schoenwolf *et al.*, 1992; Tam and Beddington, 1992).

While the notochord ingresses through the node at the anterior end of the streak in the chick and the mouse, it involutes intact around the dorsal blastopore lip in urodeles, remaining part of the epithelial lining of the gastrocoel until late neurulation. In this regard, urodele gastrulation is more like that of the reptile, which has an open dorsal blastopore through which the presumptive superficial notochord involutes (see references in Nelsen, 1953), rather than that of chick or mouse, which gastrulate strictly by ingression (Bellairs, 1986; Lawson *et al.*, 1991; Schoenwolf *et al.*, 1992; Tam and Beddington, 1992; Sulik *et al.*, 1994). It appears that the mouse reforms, or re-epithelializes, an epithelial notochord on the roof of the gastrocoel, and that

this superficial notochord later ingresses, de-epithelializing again, and is covered over by the definitive endoderm (Sulik *et al.*, 1994). In this regard, it resembles the urodele. However, it is not known how the ingressing endoderm or notochordal mesoderm, in the case of the mouse, reforms an epithelium in amniotes. Reptiles should be a fruitful system for studying the evolution of the primitive streak and the blastopore and illuminating the differences and similarities between amphibian and amniote.

Thus, the mechanism of mesodermal internalization (ingression) is unexpectedly similar in urodeles and amniotes, whereas the geometry of germ layer rearrangement varies. We hypothesize that the ingression mechanism found in urodeles has been conserved in amniotes, while the geometry has been modified to suit amniote embryonic structure and that the urodele's bilateral primitive streak may represent an early intermediate in the evolution of the amniote primitive streak from the anamniote blastopore.

Mechanism of Subduction

Subduction involves an EMT, and it is not known how epithelial cells leave an epithelial sheet while maintaining the mechanical and physiological integrity of the epithelium in this or any other system. These subducting urodele mesoderm cells may minimize the problem of withdrawal from the epithelial layer by reducing their apical membrane and, coordinately, their apical junctional complex during apical constriction. Internalized biotin-labeled membrane in the necks of the ingressing and recently ingressed bottle cells may represent apical membrane and junctional complex endocytosed together at the margins of the cell. Electron microscopy shows that large numbers of vesicles appear in the necks of the forming bottle cells in amphibians (Balinsky, 1961; Baker, 1965; Perry and Waddington, 1966; Schroeder, 1970; Lofberg, 1974).

Excess cingulin may be removed from the apical tight junctional complexes as the apical circumferences of the cells decrease, as cingulin immunoreactivity is also observed in the necks of the bottle cells. Or cingulin may be pulled down the necks of constricting bottle cells if the tight junctions become elongated perpendicular to the apical surface, as seen in mammary epithelial cells (Pitelka and Taggart, 1983). Little is known about the disassembly or dissociation of epithelial cell junctions, and especially tight junctions, during EMT (reviewed in Mercer, 2000) in any system, and even less is known about the process in developing embryos (e.g., Revel *et al.*, 1973). Endocytosis has been suggested as a mechanism involved in the regulation of desmosomal, and especially adherens junctional components during epithelial morphogenesis (Burdett, 1993; Fink and Cooper, 1996; Miller and McClay, 1997; Kamei *et al.*, 1999; Le *et al.*, 1999; Palacios *et al.*, 2001). However, tight junctions apparently disassemble only slowly on de-epithelialization (e.g., Revel *et al.*, 1973; Pitelka *et al.*, 1983) and may initially only change their functional state, as is the case for the regulation of tight

junction function in mammary glands (reviewed in Nguyen and Neville, 1998).

Complete removal of cingulin and the tight junctional complex is not required for subduction. The fact that cingulin is present in an apical band up to the point of ingression shows that cells do not lose their epithelial character as they approach the SZ. And many, apparently recently ingressed deep, bottle-shaped cells continue to show cingulin immunoreactivity at their former apical ends. Moreover, apical constriction is not obligatory for ingression, as some cells, at least in our explants, appear to approach and go through the SZ without ever fully constricting their apices.

Ingressing cells disappear beneath an advancing epithelial sheet, which nevertheless seems to be attached to the ingressing cells at the point of ingression (in the SZ, where the mesoderm meets the endoderm). How might cells detach from the epithelium while maintaining epithelial continuity? One possibility is that junctions between neighboring cells zip together as the apex of the ingressing cell is decreased to the vanishing point. In this case, epithelial disruption could be minimized by rapid formation of junctions between remaining epithelial cells as the apex of the ingressing cell is removed. Alternatively, these new junctions might be formed *over* the ingressing cell, between the adjacent endodermal and uningressed mesodermal cells. In this case, new junctions would arise within the apical region of the newly joining cells and a transient double tight junctional layer would form, bridging over the ingressing cell. These cells would thus have an adhesive apical surface, while still part of an epithelium. In the case of ingressing cells with constricted apices, this would involve very small protrusions, but in cases of cells ingressing without complete apical constriction, large bridging lamellipodia might be involved. This is suggested by our unsubstantiated observations of endodermal lamellipodia reaching over ingressing cells.

Patterning of Subduction: Progressive De-epithelialization and Ingression and Autonomy of De-epithelialization

De-epithelialization is a locally autonomous process within the IMZ as shown by the comparable loss of epithelial behavior and expression of mesenchymal protrusive activity isolated lateral IMZs. Neither vegetal contact with the endoderm nor dorsal contact with Spemann's organizer is necessary after the onset of gastrulation. However, this does not preclude an earlier signal from either or both of these regions. Within the IMZ, de-epithelialization may be cell autonomous at the early gastrula stage, or it may be organized by signals internal to the IMZ during gastrulation.

De-epithelialization is not dependent on the cells being able to actually ingress into a deep region and to crawl away once they have become mesenchymal, as this process will occur in place, with the dissociated cells remaining super-

ficial, when subduction is prevented. But the fact that de-epithelialization under these conditions occurs later than subduction in giant sandwich explants and intact embryos suggests that de-epithelialization is normally coordinated with ingression. The timing of de-epithelialization is probably normally regulated by the actual ingression event, such that the cells coordinate their progressive loss of epithelial characters with subduction. The early loss of some epithelial characters may be necessary for subduction since the cell behaviors characteristic of stable epithelia, including contact paralysis of movement and apical junction formation (Middleton, 1972, 1977; Brown and Middleton, 1987), assure maintenance of a sheet of cells, rather than allowing ingression. The cells normally adopt mesenchymal behaviors, such as cell migration or intercalation once they have completed ingression, and some regulatory checkpoint presumably prevents this from occurring too early in the unperturbed embryo. But the cells have apparently been started on an inevitable road to de-epithelialization, and so when subduction does not occur in our restricted explants, eventually the surface cells by-pass this control and de-epithelialize anyway. Obviously it would be disadvantageous to complete de-epithelialization prior to the capacity of the cells to ingress into the deep region. If the two were not coupled and de-epithelializing cells were not also ingressing, the remaining epithelial cells could not reseal the epithelial barrier protecting the inside of the embryo from the vicissitudes of external conditions. We would like to determine the origin of the signal setting the de-epithelialization process in motion, and to determine whether blocking de-epithelialization in LMZ explants also blocks subduction.

Progressive De-epithelialization Follows the Anterior-to-Posterior and Lateral-to-Medial Master Pattern Generator in Amphibians

In *X. laevis*, the mediolateral intercalation behavior (MIB) that drives convergent extension is expressed in a pattern that begins in the presumptive lateral anterior somitic mesoderm. It then progresses posteriorly along the presumptive lateral edge of the future somitic mesoderm, and from this lateral origin, it spreads medially toward the boundary with the notochord. Likewise, MIB spreads posteriorly along the lateral edge of the presumptive notochord, and from this lateral origin, it spreads medially (Keller *et al.*, 1992; Shih and Keller, 1992).

Here, in the urodeles, we show that subduction behavior of the superficial presumptive mesoderm spreads in a very similar pattern within the marginal zone, originating along the vegetal edge of the presumptive somitic region and spreading away from that edge (see Fig. 5E, black arrows). In the presumptive somitic tissues, this behavior spreads toward the notochord, resulting in the observed juxtaposition of the sub-blastoporal endoderm with the notochord. In the presumptive lateral-ventral mesoderm, however, the progression of subduction behavior spreads toward the

presumptive posterior ventral ectoderm, such that the most ventral sub-blastoporal endoderm comes to lie adjacent to it, rather than the notochord.

Urodeles Are a Useful Model System

The urodeles are a fruitful system in which to study the cellular mechanisms of ingression and EMT. Cells move into the deep layers at roughly 40 $\mu\text{m}/\text{h}$, with one cell taking 20–40 min to ingress. This suggests relatively rapid changes in expression and/or activity of adhesion molecules, cell matrix receptors, cytoskeletal components, and the regulatory pathways of each in these cells. Adhesion molecules that were keeping these cells integrated into the epithelium must be exchanged for those that will allow them to interact with the cells and matrix molecules in their new deep environment. Tight junctions and desmosomes must be disassembled. Similarly dramatic changes must occur inside the cell, as the cytoskeleton and other cellular components change from an epithelial to a mesenchymal organization.

Unexpectedly, urodele gastrulation also shares much more than we would have expected with amniote gastrulation as both involve massive de-epithelialization and ingression. In contrast, anurans in general make less use of these processes; most notably, *Xenopus*, which is the dominant amphibian model system, makes little use of these important morphogenic processes.

ACKNOWLEDGMENTS

We thank Adam Jones for the *T. granulosa*, Bess Murray and Lyle Zimmerman for showing us where to find *A. maculatum*, and the Indiana University axolotl colony for *A. mexicanum*. We thank Linda Barlow, Erica Crespi, and Lance Davidson for helpful comments on the manuscript. This research was supported by NIH NRSA 5-F32-HD08183 (to D.R.S.) and NIH RO1 HD 25594 and RO1 HD 36426 (to R.K.).

REFERENCES

Baker, P. C. (1965). Fine structure and morphogenic movements in the gastrula of the treefrog, *Hyla regilla*. *J. Cell Biol.* **24**, 95–116.

Balinsky, B. I. (1961). Ultrastructural mechanisms of gastrulation and neurulation. In pp. 550–563. Institut Internationale Zdz'znnospacezzembryologiezz and Fondazione A. Baselli, Palanza.

Bellairs, R. (1986). The primitive streak. *Anat. Embryol. (Berl.)* **174**, 1–14.

Bordzilovskaya, N. P., Dettlaff, T. A., Duhon, S. T., and Malacinski, G. M. (1989). Developmental-stage series of axolotl embryos. In "Developmental Biology of the Axolotl" (J. B. Armstrong and G. M. Malacinski, Eds.), Oxford Univ. Press, New York.

Brown, R. M., and Middleton, C. A. (1987). Contact behaviour during the reassociation of dissociated epithelial cells in primary culture. *J. Cell Sci.* **88**, 521–526.

Burdett, I. D. (1993). Internalisation of desmosomes and their entry into the endocytic pathway via late endosomes in MDCK cells:

Possible mechanisms for the modulation of cell adhesion by desmosomes during development. *J. Cell Sci.* **106**, 1115–1130.

Cardellini, P., Davanzo, G., and Citi, S. (1996). Tight junctions in early amphibian development: Detection of junctional cingulin from the 2-cell stage and its localization at the boundary of distinct membrane domains in dividing blastomeres in low calcium. *Dev. Dyn.* **207**, 104–113.

Citi, S. (1992). Protein kinase inhibitors prevent junction dissociation induced by low extracellular calcium in MDCK epithelial cells. *J. Cell Biol.* **117**, 169–178.

Davidson, L. A., and Keller, R. E. (1999). Neural tube closure in *Xenopus laevis* involves medial migration, directed protrusive activity, cell intercalation and convergent extension. *Development* **126**, 4547–4556.

Fesenko, I., Kurth, T., Sheth, B., Fleming, T. P., Citi, S., and Hausen, P. (2000). Tight junction biogenesis in the early *Xenopus* embryo. *Mech. Dev.* **96**, 51–65.

Fink, R. D., and Cooper, M. S. (1996). Apical membrane turnover is accelerated near cell-cell contacts in an embryonic epithelium. *Dev. Biol.* **174**, 180–189.

Holtfretey, J. (1944). A study of the mechanics of gastrulation. Part II. *J. Exp. Zool.* **95**, 171–212.

Imoh, H. (1988). Formation of germ layers and roles of the dorsal lip of the blastopore in normally developing embryos of the newt *Cynops pyrrhogaster*. *J. Exp. Zool.* **246**, 258–270.

Jordan, E. (1893). The habits and development of the newt. *J. Morphol.* **8**, 318–358.

Kamei, T., Matozaki, T., Sakisaka, T., Kodama, A., Yokoyama, S., Peng, Y. F., Nakano, K., Takaishi, K., and Takai, Y. (1999). Coendocytosis of cadherin and c-Met coupled to disruption of cell-cell adhesion in MDCK cells: Regulation by Rho, Rac and Rab small G proteins. *Oncogene* **18**, 6776–6784.

Keller, R. (1991). Early embryonic development of *Xenopus laevis*. *Methods Cell Biol.* **36**, 61–113.

Keller, R., Shih, J., and Domingo, C. (1992). The patterning and functioning of protrusive activity during convergence and extension of the *Xenopus* organiser. In "Development 1992 Supplement—Gastrulation" (C. D. Stern and P. W. Ingham, Eds.), pp. 81–91.

Keller, R. E. (1986). The cellular basis of amphibian gastrulation. In "Developmental Biology: A Comprehensive Synthesis. 2. The Cellular Basis of Morphogenesis" (L. Browder, Ed.), pp. 241–327. Plenum, New York.

King, H. D. (1903). The formation of the notochord in the amphibia. *Biol. Bull.* **4**, 287–300.

Lawson, K. A., Meneses, J. J., and Pedersen, R. A. (1991). Clonal analysis of epiblast fate during germ layer formation in the mouse embryo. *Development* **113**, 891–911.

Le, T. L., Yap, A. S., and Stow, J. L. (1999). Recycling of E-cadherin: A potential mechanism for regulating cadherin dynamics. *J. Cell Biol.* **146**, 219–232.

Lewis, W. H. (1948). Mechanics of *Amblystoma* gastrulation. *Anat. Rec.* **101**, 700.

Lewis, W. H. (1952). Gastrulation of *Amblystoma punctatum*. *Anat. Rec.* **112**, 473.

Lofberg, J. (1974). Apical surface topography of invaginating and noninvaginating cells: A scanning-transmission study of amphibian neurulae. *Dev. Biol.* **36**, 311–329.

Lundmark, C. (1986). Role of bilateral zones of ingressing superficial cells during gastrulation of *Ambystoma mexicanum*. *J. Embryol. Exp. Morphol.* **97**, 47–62.

- Mercer, J. A. (2000). Intercellular junctions: Downstream and upstream of Ras? *Semin. Cell Dev. Biol.* **11**, 309–314.
- Middleton, C. A. (1972). Contact inhibition of locomotion in cultures of pigmented retina epithelium. *Exp. Cell Res.* **70**, 91–96.
- Middleton, C. A. (1977). The effects of cell-cell contact on the spreading of pigmented retina epithelial cells in culture. *Exp. Cell Res.* **109**, 349–359.
- Miller, J. R., and McClay, D. R. (1997). Characterization of the role of cadherin in regulating cell adhesion during sea urchin development. *Dev. Biol.* **192**, 323–339.
- Minsuk, S. B., and Keller, R. E. (1996). Dorsal mesoderm has a dual origin and forms by a novel mechanism in *Hymenochirus*, a relative of *Xenopus*. *Dev. Biol.* **174**, 92–103.
- Minsuk, S. B., and Keller, R. E. (1997). Surface mesoderm in *Xenopus*: A revision of the stage 10 fate map. *Dev. Genes Evol.* **207**, 389–401.
- Miranda, K. C., Khromykh, T., Christy, P., Le, T. L., Gottardi, C. J., Yap, A. S., Stow, J. L., and Teasdale, R. D. (2001). A dileucine motif targets E-cadherin to the basolateral cell surface in Madin-Darby canine kidney and LLC-PK1 epithelial cells. *J. Biol. Chem.* **276**, 22565–22572.
- Mostov, K. E., Verges, M., and Altschuler, Y. (2000). Membrane traffic in polarized epithelial cells. *Curr. Opin. Cell Biol.* **12**, 483–490.
- Nelsen, O. E. (1953). "Comparative Embryology of the Vertebrates." The Blakiston Company, New York.
- Nguyen, D. A., and Neville, M. C. (1998). Tight junction regulation in the mammary gland. *J. Mammary Gland Biol. Neoplasia* **3**, 233–246.
- Palacios, F., Price, L., Schweitzer, J., Collard, J. G., and D'Souza-Schorey, C. (2001). An essential role for ARF6-regulated membrane traffic in adherens junction turnover and epithelial cell migration. *EMBO J.* **20**, 4973–4986.
- Pasteels, J. (1942). New observations concerning the maps of presumptive areas of the young amphibian gastrula. (*Amblystoma* and *Discoglossus*). *J. Exp. Zool.* **89**, 255–281.
- Perry, M. M., and Waddington, C. H. (1966). Ultrastructure of the blastopore cells in the newt. *J. Embryol. Exp. Morphol.* **15**, 317–330.
- Pitelka, D. R., and Taggart, B. N. (1983). Mechanical tension induces lateral movement of intramembrane components of the tight junction: Studies on mouse mammary cells in culture. *J. Cell Biol.* **96**, 606–612.
- Pitelka, D. R., Taggart, B. N., and Hamamoto, S. T. (1983). Effects of extracellular calcium depletion on membrane topography and occluding junctions of mammary epithelial cells in culture. *J. Cell Biol.* **96**, 613–624.
- Poznanski, A., Minsuk, S., Stathopoulos, D., and Keller, R. (1997). Epithelial cell wedging and neural trough formation are induced planarily in *Xenopus*, without persistent vertical interactions with mesoderm. *Dev. Biol.* **189**, 256–269.
- Psychoyos, D., and Stern, C. D. (1996). Fates and migratory routes of primitive streak cells in the chick embryo. *Development* **122**, 1523–1534.
- Purcell, S. M., and Keller, R. (1993). A different type of amphibian mesoderm morphogenesis in *Ceratophrys ornata*. *Development* **117**, 307–317.
- Revel, J., Yip, P., and Chang, L. L. (1973). Cell junctions in the early chick embryo: A freeze etch study. *Dev. Biol.* **35**, 302–317.
- Rugh, R. (1948). "Experimental Embryology: A Manual of Techniques and Procedures." Burgess Publishing Company, Minneapolis.
- Sater, A.-K., Steinhardt, R.-A., and Keller, R. (1993). Induction of neuronal differentiation by planar signals in *Xenopus* embryos. *Dev. Dyn.* **197**, 268–280.
- Schoenwolf, G. C., Garcia, M.-V., and Dias, M. S. (1992). Mesoderm movement and fate during avian gastrulation and neurulation. *Dev. Dyn.* **193**, 235–248.
- Schroeder, T. E. (1970). Neurulation in *Xenopus laevis*: An analysis and model based upon light and electron microscopy. *J. Embryol. Exp. Morphol.* **23**, 427–462.
- Shih, J., and Keller, R. (1992). Patterns of cell motility in the organizer and dorsal mesoderm of *Xenopus laevis*. *Development* **116**, 915–930.
- Sulik, K., Dehart, D. B., Inagaki, T., Carson, J. L., Vrablic, T., Gesteland, K., and Schoenwolf, G. C. (1994). Morphogenesis of the murine node and notochordal plate. *Dev. Dyn.* **201**, 260–278.
- Tam, P. P., and Beddington, R. S. (1992). Establishment and organization of germ layers in the gastrulating mouse embryo. *Ciba Found. Symp.* **165**, 27–41; discussion 42–49.
- Vogt, W. (1929). Gestaltungsanalyse am Amphibienkiem Mit Ortlicher Vitalfärbung. II. Teil. Gastrulation und Mesodermbildung Bei Urodelen und Anuren. *Wilhelm Roux Arch. Entwicklungsmech. Org.* **120**, 384–601.
- Wilson, P. (1990). The development of the axial mesoderm in *Xenopus laevis*. In "Zoology." University of California, Berkeley.
- Wilson, P. A., Oster, G., and Keller, R. (1989). Cell rearrangement and segmentation in *Xenopus*: Direct observation of cultured explants. *Development* **105**, 155–166.

Received for publication December 26, 2001

Revised April 26, 2002

Accepted May 1, 2002

Published online July 9, 2002